JOURNAL OF MATERIALS SCIENCE **34** (1999) 5847–5851

Effect of applied potential on the nature of surface film and SCC of a high Mn stainless steel in 1 M HCl

A. DEVASENAPATHI*, M. ASAWA
Graduate School, Faculty of Education, Shinshu University, Nishi-Nagano, Nagano-380, Japan
E-mail: masawa1@gipwc.shinshu-u.ac.jp

The Stress Corrosion Cracking (SCC) behavior of a high Mn austenitic stainless steel (SS) with 14.67 wt % Mn was studied in 1 M hydrochloric acid at room temperature as a function of potential. At open circuit potential (OCP) thick black surface film formation and a transgranular mode of cracking were observed. At all applied anodic potentials general dissolution and ductile cracking were observed. X-ray photoelectron spectroscopy (XPS) studies were conducted to characterise the surface films formed at different potentials. The nature of the surface film was found to be different with a change in potential. The nature of the film formed was found to govern the dissolution behavior and therefore the fracture morphology of the alloy.

1. Introduction

Studies on the stress corrosion cracking (SCC) behavior of austenitic stainless steels with 18Cr-8Ni in acidic chloride solutions are numerous [1–8]. Studies indicate that the SCC susceptibility of type 304 stainless steel depends on the pH, chloride ion (Cl^-) concentration and potential [1–3, 6]. Theories have been proposed based on the adsorption of Cl^- which results in a nonprotective film formation and incomplete inhibition of the active dissolution of the base metal [7]. Fang *et al*. [8] have reported that SCC occurs at active potentials where a moderately protective film enriched with Cr and Ni is formed. The breakdown of this film is reported to initiate a transgranular (TG) mode of cracking in type 304 stainless steel in acidic chloride environments. While the role of alloying elements such as Cr and Ni in SCC have been studied [9, 10] extensively, the role of Mn is not well known. The role of Mn in SCC is significant because of the interest in the development and use of high Mn stainless steels with partial or complete replacement of Ni as an austenite stabiliser [11]. These high Mn stainless steels provide not only superior strength and nonmagnetic properties but also lower the cost of the alloy to a considerable extent. Earlier studies with a 9 wt % Mn stainless steel indicated that the SCC behavior of these stainless steels are different than type 304 stainless steel [12]. The surface film formed was found to have a crucial role in governing the SCC behavior of the high Mn stainless steel. However, the studies on the nature of corrosion films formed on high Mn stainless steel are sparse [13]. Therefore, the present study was undertaken to study the nature and role of the surface film in SCC of a 14.58 at % Mn stainless steel designated as 8S.

2. Experimental

For the present study a high Mn stainless steel (8S) and type 304 stainless steel of composition shown in Table I was used. Polarisation studies were carried out using specimens of 1 cm^2 surface area and SCC tests using wires of dimension 1×1 mm (regular square) in cross section. The specimens were solutionised at a temperature of 1100 °C in argon atmosphere for 1 h and quenched by a sudden flow of argon gas at room temperature. The specimens were abraded to 600 grit finish using silicon carbide papers, washed in acetone followed by distilled water and dried in hot air. One molar HCl prepared from AR grade chemical and deionised water was used as the test environment. The specific conductivity of the water was <0.2 μS/cm. Polarisation studies were conducted using a potentiostat at a scan rate of 20 mV per minute using saturated calomel as the reference and Pt foil as the counter electrode. SCC tests were carried out in a cantilever type constant load set up. The details of the experimental set-up have been described elsewhere [14]. Both the polarisation and SCC studies were conducted at room temperature. For SCC the specimens were tested at 75% yield strength of the alloy which was 265 MPa and the time taken for complete fracture of the specimen was taken as the time to failure. The effect of external potential on SCC behaviour was also studied. The specimens were maintained at the required potential using a potentiostat with a saturated

* *Present Address*: Graduate School, Faculty of Engineering, Shinshu University, 500 Wakasato, Nagano—380.

TABLE I Chemical composition of stainless steels used for the present study (at %)

Element	8S	Type 304
C	0.250	0.242
Si	0.656	1.04
P	0.038	0.056
S	0.011	0.024
Ni	1.14	8.130
Cr	17.89	19.54
Mn	14.58	0.99
Cu	0.092	0.043
Mo	0.108	0.080
N	1.47	—

calomel as the reference and Pt foil as the counter electrodes respectively. The nature of the film formed on the alloy was characterised using XPS. XPS analysis was conducted in an ULVAC-PHI 5600 Model X-ray photo electron spectrometer. For XPS studies 5×5 mm size specimens cut from sheets of 1 mm thickness were used. The film was allowed to form at three different potentials, the open circuit potential (OCP), −200 mV and 0 mV vs. SCE in 1 M HCl for 30 min. The specimens were immediately transferred into the vacuum chamber of the XPS setup. XPS spectra was obtained using an X-ray source operated at 14 keV energy and 20 mA emission current using MgK_α radiation. Depth profiling of the film was performed by sputtering with Ar^+ ions of 2 keV energy for 5 min at an approximate rate of 1 nm/min. The spectra obtained were smoothed by a modified Sherwood method to minimise truncation errors. Deconvolution was done using a curve fitting program with background subtraction. Quantitative analysis was performed by taking into account of the atomic sensitivity factors of the elements as described [15].

3. Results

3.1. Polarisation

The polarisation behavior of 8S alloy in 1 M HCl is shown in Fig. 1. In order to understand the effect of high Mn on polarisation, the curve is compared with that of type 304 stainless steel. Compared to type 304

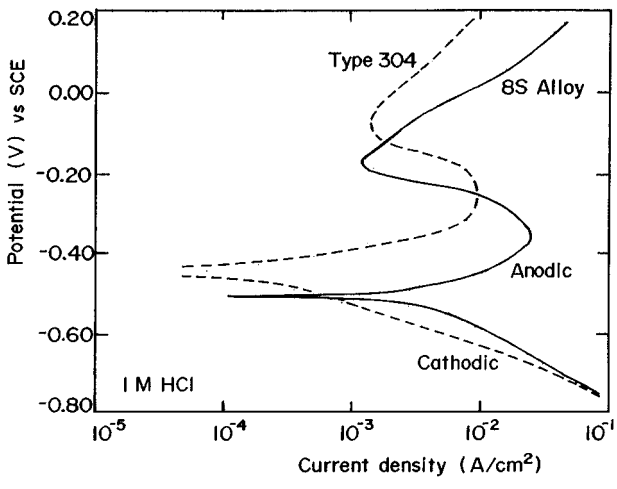

Figure 1 Comparision of polarisation behavior of 8S and type 304 stainless steels.

TABLE II SCC test results of 8S alloy tested at 75% of its yield strength in 1 M HCl with change in potential

Potential, mV vs. SCE	Time to failure (h)	% Reduction in area
OCP	4	38
−400	3.5	49
−300	2.5	67
−200	2	69
−100	2	73
0	1.5	75

stainless steel 8S alloy exhibits a −100 mV shift in OCP in the cathodic direction indicating that the cathodic hydrogen evolution reaction is favoured for the 8S alloy. The anodic polarisation curve shows a higher critical current density (i_{crit}) value of 25 mA/cm^2 for the 8S alloy; type 304 stainless steel exhibits a value of 9 mA/cm^2. A very narrow passive range indicating inadequate passivation for the 8S alloy which is similar to type 304 stainless steel is observed. Polarisation towards more anodic potentials leads to an increase in the current density indicating a higher dissolution rate of the 8S alloy.

3.2. SCC

The SCC results of the 8S alloy tested at 75% of its yield strength at different externally applied anodic potentials are shown in Table II. The table shows a steady decrease in time to failure starting from OCP with applied anodic potentials. While the specimen fractured in 4 h at OCP, the time to fracture decreased to 1.5 h at 0 mV. The test solution turned green during testing indicating a higher dissolution tendency of the alloy in 1 M HCl at all potentials. While a thick black surface film formation was observed at OCP, no such thick film was observed at anodic potentials. On the other hand, the surface of the specimens tested at anodic potentials were rough indicating general dissolution. The % reduction in cross sectional area of the specimens from its original cross section after fracture is given in Table II. While the reduction in area of the specimen that failed at OCP is only 38%, the value increases steadily with applied anodic potential. This indicates a higher dissolution tendency of the alloy at anodic potentials as stated above.

3.3. Fractography

The fracture morphology of specimens that failed at different potentials is shown in Fig. 2a–d. Fig. 2a shows the fracture surface of the specimen failed at OCP, which is clearly transgranular. Fig. 2b–d show the fracture surfaces of specimens that failed at −400, −200 and 0 mV respectively. All the fractographs (Fig. 2b–d) show features of extensive general corrosion at the edges and dimples due to overload failure at the center.

3.4. ESCA

ESCA spectra obtained on the corrosion film formed on Mn stainless steel at OCP is shown in Fig. 3, which

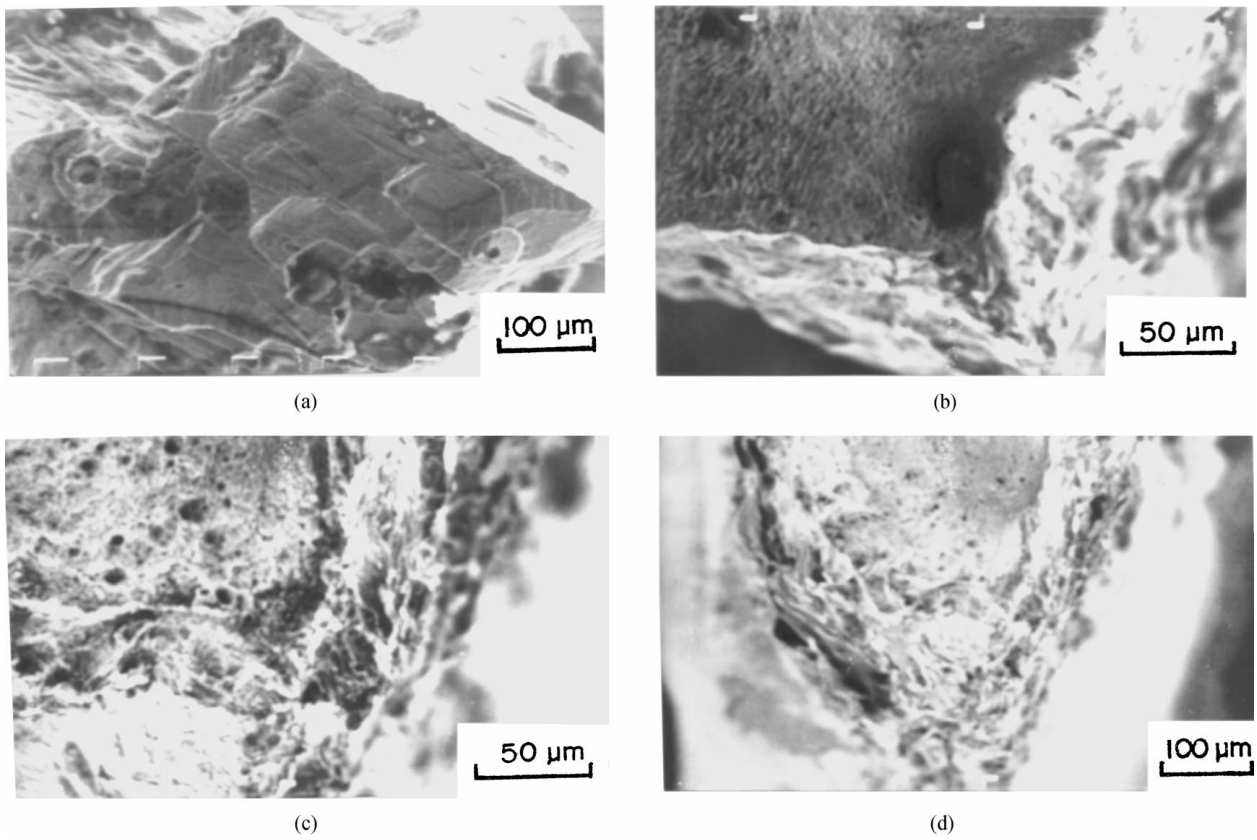

Figure 2 Fractographs of 8S alloy failed at (a) OCP showing a transgranular mode of cracking, (b) −400 mV, (c) −200 mV and (d) 0 mV showing general dissolution at the edges and dimples at the center.

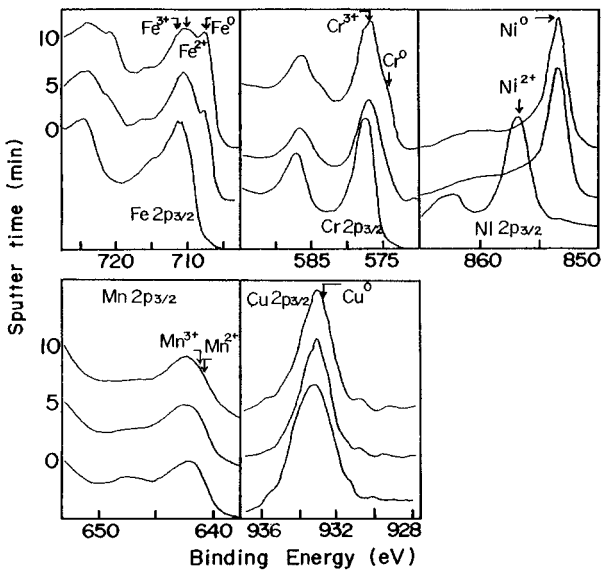

Figure 3 XPS spectra of film formed at OCP with change in sputtering time for various elements.

shows the individual spectra obtained for various metallic elements vs. sputtering time. From the binding energy (BE) values [16, 17], it is noted that Fe is present in both Fe^{2+} (709.9 eV) and Fe^{3+} (711.6 eV) forms in the corrosion films formed at all potentials. With sputtering the Fe^0 (706.9 eV) component is found to increase in concentration. Also, Cr is present in the form of Cr^{3+} (576.8 eV) [17] in the top layers with its presence in the metallic state Cr^0 (574 eV) to a lower extent in the inner layers. Further, it is noted that Ni is present in its oxidised state as Ni^{2+} (857 eV) at the top surface of the film while its presence only in the elemental state Ni^0 (853.5 eV) is observed with sputtering [17]. From this it can be concluded that Ni is oxidised to a lesser extent from the alloy or Ni is reduced in the film. Mn is present in the form of Mn^{2+} (640.8 eV) and Mn^{3+} (641.2 eV) throughout the film. Since the BE of Cu^0 and Cu_2O vary only by a value of 0.1 eV (932.7 eV) it is difficult to determine the actual state of Cu [18] from the spectra. However, Cu can be expected to deposit as CuO (932.7 eV) as its standard potential is more positive than the anodic potentials employed.

The spectra obtained for oxygen O1s shows the presence of oxygen in the form of oxides M─O (530.5 eV), hydroxide and oxyhydroxide (M─OH, M─O─O─H) (531.8 eV) and combined with water H─O─H (532.2 eV) [19]. Further, the shift in the peak towards higher BE values (532.2 eV) observed in the top layers indicates the presence of a large amount of water. With sputtering the peak shifts towards lower BE values indicating a decreasing water content in the film and an increase in the oxide, hydroxide and oxyhydroxide contents. The presence of chloride in both $Cl2p_{3/2}$ (200.4 eV) and $Cl2p_{1/2}$ (198.4) states is observed throughout the film [19].

The atomic % (at %) concentration of individual metallic elements present in the film has also been calculated. The change in at % concentration of individual elements with potential and sputtering time is shown in Fig. 4. It is observed that the concentration of Fe does not vary significantly with potential. However, Fe increases in the inner layers of the corrosion film. The

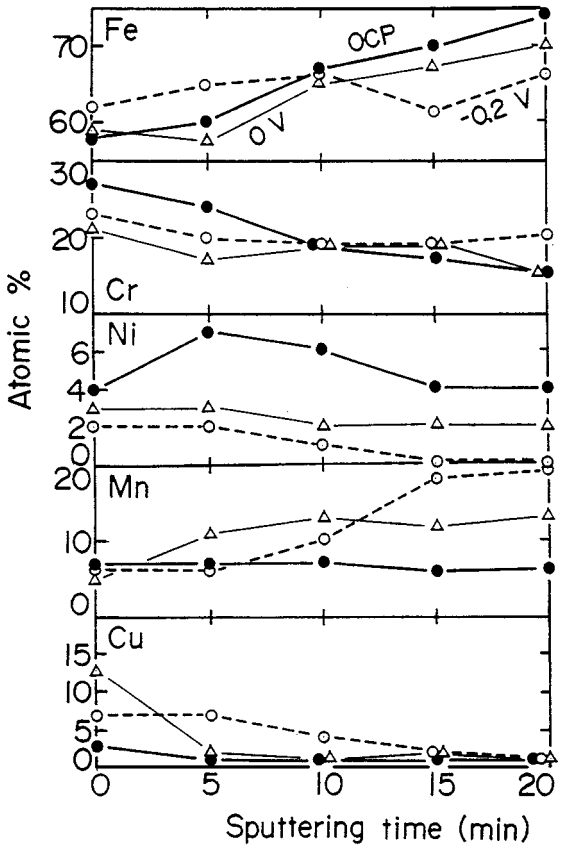

Figure 4 The variation in at % concentration of metallic elements with change in potential and sputtering time.

film formed at OCP shows a Cr content of 27 at % at the top surface which decreases with sputtering. This is higher than, the concentration of Cr present in the films formed at −200 and 0 mV. The Ni content of the film formed is also found to be higher at OCP which decreases at −200 and 0 mV. The Mn content of the film formed at −200 and 0 mV increases with sputtering indicating an enrichment of this element, while Cu is enriched at the surface.

In order to determine the approximate thickness of the corrosion films formed, after the XPS analysis which used 20 min sputtering at an energy of 2 keV, final sputtering was carried out at an energy of 4 keV. The base metal could be reached after sputtering for 5 min in the case of films formed at −200 and 0 mV. For films formed at OCP, even sputtering for 20 min at 4 keV was insufficient to sputter through the film as observed by the presence of O1s and $Cl2p_{3/2}$. This indicates the film formed at OCP is several order of magnitude thicker as observed from the visible black surface film formed during testing.

4. Discussion

The test results and fractographs of the specimens show that the 8S alloy undergoes SCC failure at OCP in 1 M HCl. An increase in the dissolution tendency with a resultant ductile failure is observed at all the anodic potentials tested. The presence of a thick black surface film at OCP and the absence of such a thick film with a resultant ductile failure at anodic potentials indicate that the thick surface film formed in 1 M HCl has a crucial role in determining the SCC susceptibility of the alloy. In order to have a comprehensive understanding of the nature of the surface film and its influence on the fracture behavior, the XPS results obtained at OCP are compared with that of (i) the literature already reported on the nature of film formed on stainless steels in acidic chloride environments and (ii) with the XPS results obtained at −200 and 0 mV.

In stainless steels, the enrichment of Cr in the surface film is known to help in reducing the corrosion of the base alloy. The selective dissolution of Fe from the oxide film is reported to result in Cr enrichment [20–23]. Studies by Olefjord [23] show that the films formed on austenitic stainless steel in acidic chloride solution are enriched in Cr to 60 at % at the passive potentials which decreases by two fold at active potentials. The Cr content of the film formed on 8S alloy is low at all potentials compared to the values reported for austenitic stainless steels (Fig. 4). It is reported that Ni is in general enriched below the surface film as it is relatively more noble, and it enhances the passivation tendency of the base alloy [17, 23–25]. However in the case of 8S alloy, it is to be noted that Ni is not only retained below the film but present throughout the film. While, Ni is present in its oxidised state at the top surface, it exists in elemental form in the inner layers. Also, the Fe content shows a minimum of 58 at % which is higher than the 30 at % reported for austenitic stainless steel in acidic chloride solutions [25].

The lowering of Cr content, the increase in Fe content and the presence of Ni throughout the film implies that the films formed on the 8S alloy are different than that formed on type 304 stainless steel. As the Ni content of the base alloy is very low (1.14 at %) in the case of 8S alloy, a possible role of low Ni in decreasing the film stability can be expected. But it should be emphasised that ferritic stainless steels without Ni also form films with Cr enrichment to the extent observed in type 304 stainless steel [13] with 8 wt % Ni in 1 M HCl. Therefore the change in the nature of films formed can be attributed to the presence of electrochemically more active Mn present at 14.58 at % in the base alloy. It is worthwhile to mention that previous study [26] also indicated the lowering of film stability by the presence of Mn oxides in the case of Fe-Mn-Al-Cr alloy. Thus the typical film formation by the oxidation of alloying elements from the base metal and the selective dissolution of more active Fe oxides from the film causing enrichment of Cr as observed in the case of type 304 stainless steel may not be occurring in the 8S alloy. Rather a semiprotective film formation by the initial oxidation of alloying elements into the solution due to the presence of higher amount (14.58 at %) of electrochemically more active Mn is expected. So, further dissolution of the base alloy could take place at sites where there is film breakdown. As the film grows the potential of the inner portions of the film is decreased where as the metal-liquid interface is at the controlled potential. This decrease in potential during film growth in the inner regions of the film could result in the reduction of the oxidised metal constituents

dissolving from the base alloy. The presence of Ni and Cu in their elemental state further confirm these propositions. This proposition gains further support from the XPS studies [26] of films formed on Fe-Mn-Al-Cr alloys which show the presence of alloying elements as their oxides and hydroxides at the outersurface and in their elemental state inbetween the film and the substrate.

The variation in at % concentration of elements in the films formed at different potentials shows that the nature of the film formed at OCP is different than those formed at −200 and 0 mV. The higher Cr and Ni and lower Cu and Mn contents observed for films formed at OCP (Fig. 4) shows that the dissolution at OCP is rather low or the film formed helps in reducing dissolution. The reduction in protective quality of the films formed at −200 and 0 mV is further supported by polarisation and % reduction in cross sectional area values which indicate that at anodic potentials the alloy tends to be more reactive. Thus the moderately protective film formed at OCP could fracture under stress, leaving the base alloy exposed resulting in localised dissolution and SCC. Whereas, at anodic potentials since the dissolution rate is very high as indicated by the polarisation curves, a sharp crack could not be maintained resulting in a ductile failure. It is worthwhile to mention that the type 304 stainless steel has been reported to undergo a transgranular mode of cracking not only at OCP, but also at anodic potentials which extends well above the pitting potential. The ductile failure exhibited by the high Mn stainless steel at anodic potentials is attributed to the presence of electrochemically more active Mn which alters the film characteristics enhancing the dissolution of the base ally. The present study shows that the change in nature of the surface film can alter the dissolution behavior of the base alloy and therefore the fracture mode. A moderate dissolution at film breakdown sites can grow into sharp cracks resulting in SCC, while higher dissolution rates tend to result in a ductile failure.

5. Conclusions

The present study results are summarised as follows

1. 8S alloy in 1M HCl was susceptible to SCC only at OCP. At anodic potentials no SCC was observed. However, an increased dissolution leading to thinning of the specimen with a resultant ductile failure was observed.

2. ESCA studies showed the nature of surface film formed on 8S alloy different than that reported for type 304 stainless steels. The film formed on 8S alloy was found to be low in Cr content and high in Fe contents compared to the film formed on type 304 stainless steels.

3. The film formed on 8S alloy at OCP was found to be higher in Cr and Ni contents compared to the films formed at anodic potentials. While this increase in Cr and Ni contents in the film formed at OCP was attributed to an increased film stability and SCC, the decrease in Cr and Ni contents observed at anodic potentials was attributed to a higher dissolution rate and a ductile fracture.

References

1. G. BIANCHI, F. MAZZA and S. TORCHIO, *Corros. Sci.*, **13** (1974) 165.
2. J. R. GALVALE, S. B. DE WEXLER and I. GARDIAZABAL, *Corrosion* **31** (1975) 352.
3. S. TORCHIO, *Corros. Sci.* **20** (1980) 555.
4. I. MAIER and J. R. GALVALE, *Corrosion* **36** (1978) 177.
5. Z. SZKLARSKA-SMIALOWSKA and N. LUKOMSKI, *ibid.* **36** (1978) 177.
6. R. NISHIMURA, *ibid.* **46** (1990) 311.
7. G. HERBSLEB and F. THEILER, *Werkst. Korros* **49** (1989) 469.
8. Z. FANG, Y. WU, R. ZHU, B. CAO and F. XIAO, *Corrosion* **50** (1994) 873.
9. R. M. LATANISION and R. W. STAEHLE, in "Fundamental Aspects of Stress Corrosion Cracking," edited by R. W. Staehle, A. J. Forty and Von Rooyen (Houston, TX: NACE, 1969) p. 214.
10. A. J. SEDRIKS, "Corrosion of Stainless Steels : Stress Corrosion Cracking," (John Wiley & Sons, New York, 1979) p. 139.
11. P. RAMA RAO and V. V. KUTUMBA RAO, *Int. Met. Rev.* **34** (1989) 69.
12. A. DEVASENAPATHI, R. C. PRASAD and V. S. RAJA, *Scripta. Metall.* **33** (1995) 233.
13. A. DEVASENAPATHI, P. VELUCHAMY, H. MINOURA and V. S. RAJA, Corrosion (Revised and communicated).
14. M. ASAWA, *Corrosion* **46** (1990) 823.
15. JOHN F. MOULDER, WILLIAM F. STICKLE, E. SOBOL, and KENNETH D. BOMBEN, in "Hand book of X-ray Photo Electron Spectroscopy," edited by Jill Chastain, (Perkin-Elmer Corporation, America, 1992) p. 25.
16. K. HASHIMOTO and K. ASAMI, *Corros. Sci.* **19** (1979) 251.
17. B. ELSENER, D. DEFILIPPO and A. ROSSI, European Symp. Proc., edited by P. Marcus, B. Baroux and M. Keddam, (European Federation of Corrosion Publications, No. 12, 1994) p. 6.
18. L. T. TSITSOPOULOS, I. A. WEBSTER and T. T. TSOTSIS, *Surface Sci.* **220** (1989) 391.
19. K. SUGIMOTO and Y. SAWADA, *Corros. Sci.* **17** (1977) 425.
20. K. ASAMI, K. HASHIMOTO, T. MATSUMOTO and S. SHIMODAIRA, *ibid.* **16** (1976) 909.
21. K. ASAMI, K. HASHIMOTO and S. SHIMODAIRA, *ibid.* **18** (1978) 151.
22. A. R. BROOKS, C. R. CLAYTON, K. DOSS and Y. C. LU, *J. Electrochem. Soc.* **133** (1989) 2459.
23. I. OLEFJORD, *Mater. Sci. Eng.* **42** (1980) 161.
24. K. ASAMI and K. HASHIMOTO, *Corros. Sci.* **19** (1979) 1007.
25. I. OLEFJORD and BENGT-OLOF ELFSTROM, *Corrosion* **38** (1982) 46.
26. X. M. ZHU and Y. S. ZHANG, *Corrosion* **54** (1998) 3.

Received 31 July 1998
and accepted 20 April 1999